Available online at www.sciencedirect.com
SCIENCE DIRECT®
Journal of Sound and Vibration 268 (2003) 731–749
JOURNAL OF SOUND AND VIBRATION
www.elsevier.com/locate/jsvi

Chaos synchronization of a horizontal platform system

Zheng-Ming Ge*, Tsung-Chih Yu, Yen-Sheng Chen

Department of Mechanical Engineering, National Chiao Tung University, 1001 Ta Hsuej Road, Hsinchu 30050, Taiwan, Republic of China

Received 13 May 2002; accepted 10 December 2002

Abstract

Chaos and chaos synchronization of the horizontal platform system are studied in this paper. Because of the non-linear terms of the systems, the systems exhibit both regular and chaotic motions. By applying various numerical results, such as phase portraits, Poincaré maps, time history and power spectrum analysis, the behaviors of the periodic and chaos synchronization are presented. The effects of the change of parameters in the system can be found in the bifurcation diagrams. Chaos synchronization of feedback methods in two coupled systems has been studied by Lyapunov exponent and coupling strength. Besides, phase effect of external excitations and the transient time in unidirectional synchronization also have been researched.

1. Introduction

Chaos synchronization has increasing potential of applications. In conventional communication systems, sinusoidal signals are used as carriers, which normally offer excellent bandwidth efficiency. However, their transmitted power is concentrated within a narrow band, resulting in high power spectra density. Then it may lead to loss of synchronization, high interception possibilities, etc. On the contrary, chaotic signals are usually broadband and noiselike. Hence, synchronized chaotic systems can be used as cipher generators for secure communication [1], symmetry and pattern formation, and self-organization [2].

There are many effective methods that can be used for chaos synchronization. It is achieved by adding a single coupled term or two coupling terms, and detected by Lyapunov exponent. In this paper, synchronization of feedback method in two identical non-autonomous coupled systems has been studied. Then the phase effect of two coupled systems [3] and the transient time in unidirectional synchronization also have been researched.

*Corresponding author. Tel.: +886-3-5712121; fax: +886-3-5720634.
E-mail address: zmg@cc.nctu.edu.tw (Z.-M. Ge).

0022-460X/03/$ - see front matter
doi:10.1016/S0022-460X(02)01607-3

2. Equations of the system

The system considered here is depicted in Fig. 1(a)–(b). The platform can freely rotate about the horizontal axis, which penetrates its mass center. There is an accelerometer on the platform. When the platform derivates from horizon, the accelerometer will give an output signal to the torque generator, which generates a torque to inverse the rotation of the platform about rotational axis. The equation of the system is

$$A\ddot{x} + D\dot{x} + kg\sin x - \frac{3g}{R}(B - C)\cos x \sin x = F\cos \omega t, \tag{1}$$

where A, B and C are the inertia moment of the platform for axis 1, 2, and 3, respectively, D is the damping coefficient, k the proportional constant of the accelerometer, g the acceleration constant of gravity, x the rotation of the platform relative to the earth, $\alpha - \theta$ and $F\cos \omega t$ harmonic torque. The analytical analysis of this system can be seen in Ref. [4].

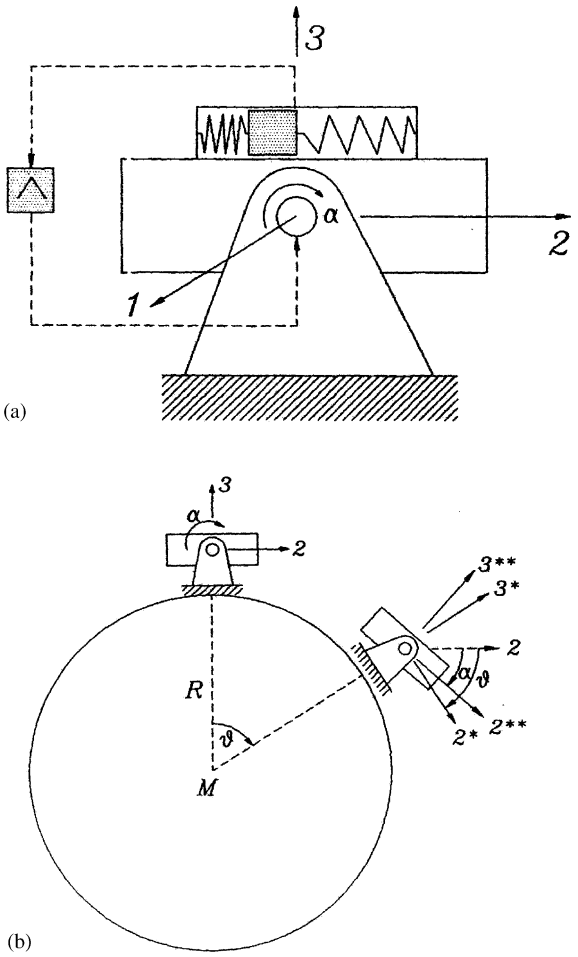

Fig. 1. (a) Physical model of the horizontal platform and (b) model of the platform circles along earth.

3. Chaos synchronization

Synchrony is the simplest effect of coupled identical oscillators: two identical oscillators display the same dynamical pattern in their common phase space. When two identical oscillators are coupled, there are only two possibilities, synchrony with no phase difference and antisynchrony with a phase difference of one-half [5].

From Eq. (1) the coupled system can be written as follows:

$$\begin{cases} \dot{x}_1 = x_2, \\ \dot{x}_2 = -\dfrac{D}{A}x_2 - \dfrac{kg}{A}\sin x_1 + \dfrac{3g}{RA}(B-C)\cos x_1 \sin x_1 + \dfrac{F}{A}\cos \omega t + F(x_3, x_1), \end{cases} \tag{2}$$

$$\begin{cases} \dot{x}_3 = x_4, \\ \dot{x}_4 = -\dfrac{D}{A}x_4 - \dfrac{kg}{A}\sin x_3 + \dfrac{3g}{RA}(B-C)\cos x_3 \sin x_3 + \dfrac{F}{A}\cos \omega t + F(x_1, x_3), \end{cases} \tag{3}$$

where $F(x_3, x_1)$ and $F(x_1, x_3)$ are coupling terms. System (2) is drive system, and system (3) is response system. These two systems are identical systems but have different initial condition.

When the oscillatory time response of two coupled chaotic oscillators are within the phase-locking range, their time response will be automatically locked to a mutual value; consequently, both systems oscillate with the same time response. In this case, they are synchronized. Various coupling terms cannot produce synchronization. Five kinds system synchronization are found with different coupling terms.

The first three driven subsystems are unidirectoional synchronization. The fourth driven subsystem is bi-directional synchronization. First, when $F(x_3, x_1) = 0, F(x_1, x_3) = k(x_1 - x_3)$ where k is coupling strength, the results are shown in Figs. 2 and 3 for the phase portrait, time-response error and drive-response diagram. Fig. 4 is Lyapunov exponent for the first driven subsystem, and Fig. 5 is synchronization time of k. In Fig. 4, when $k = 1.2$ one of the Lyapunov exponents transverse the zero value from positive to negative. This indicates that the transversality means synchronization. In Fig. 5, when k is larger than 1.2, the synchronization time is quickly reduced. The result of Fig. 6 shows that there is no synchronization in the first driven subsystem. This result means that the critical value of coupling strength k is between 1.1 and 1.2. When k is larger than critical value, synchronization would be achieved. Figs. 7–9 show the results of the second driven subsystem, in which $F(x_3, x_1) = 0$ and $F(x_1, x_3) = k\sin(x_1 - x_3)$. $F(x_3, x_1) = 0$ and $F(x_1, x_3) = k(e^{(x_1 - x_3)} - 1)$ are in the third driven subsystem. The results of the third driven subsystem are shown in Figs. 10–12. The results of the subsystems above are similar.

The bi-directional coupled system synchronization would be discussed in this section. The first bi-directional coupled system's coupling terms are $F(x_3, x_1) = k[e^{(x_3 - x_1)} - 1]$ and $F(x_1, x_3) = k[e^{(x_1 - x_3)} - 1]$. The numerical simulation results of this system are shown in Figs. 13–17. From Figs. 13, 14 and 16, we can see that when k is larger than 0.6, the system is synchronized. In Fig. 17, the transversality of Lyapunov exponent happened when $k = 0.05$. But this system does not synchronize when $k = 0.05$ (Fig. 15). This phenomenon differs from the systems shown above.

Then the coupling terms of the second bi-directional coupled system are $F(x_3, x_1) = k\sin[e^{(x_3 - x_1)} - 1]$ and $F(x_1, x_3) = k\sin[e^{(x_1 - x_3)} - 1]$, and the results are shown in Figs. 18–20. When k is larger than 0.6, the system is synchronized.

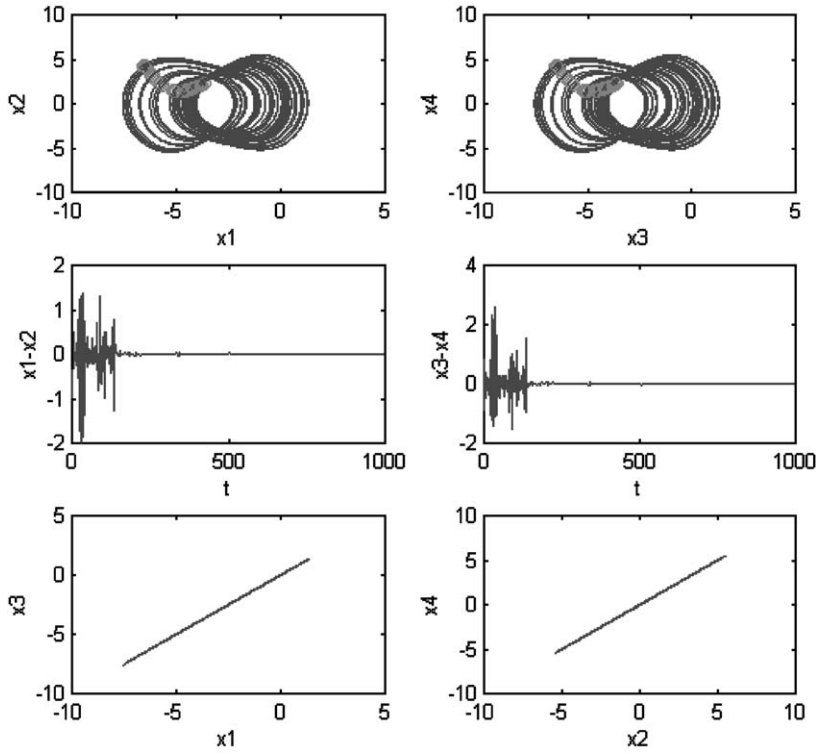

Fig. 2. Phase portraits, errors and similarity of unidirectional coupled systems with $k(x_1 - x_3)$, $k = 1.2$.

But in Fig. 20, the point $k = 0.7$ is an exceptional point, because its synchronization time is much larger than the other points nearby. So, the fourth coupled system could not be synchronized when $k = 0.7$ (See Fig. 21).

4. Phase effect of two external excitations for two coupled systems

The phase difference between external excitation may affect chaos synchronization [3]. For large difference, it even transforms the coupled oscillators from chaotic motion to regular motion.

When adding phase difference in the response system, system (3) would become

$$\begin{aligned} \dot{x}_3 &= x_4, \\ \dot{x}_4 &= -\frac{D}{A}x_4 - \frac{kg}{A}\sin x_3 + \frac{3g}{RA}(B - C)\cos x_3 \sin x_3 + \frac{F}{A}\cos(\omega t + \varphi) \\ &\quad + F(x_1, x_3), \end{aligned} \tag{4}$$

where φ is phase difference of external excitation, $0 \leqslant \varphi \leqslant 2\pi$. Now we take linear coupling term $F(x_1, x_3) = k(x_1 - x_3)$ for an example. In what follows, we fix $\omega = 1.8$ and the coupling strength $k = 50$. The bifurcation diagrams of systems (2) and (4) are shown in Figs. 22 and 23. Fig. 24 is

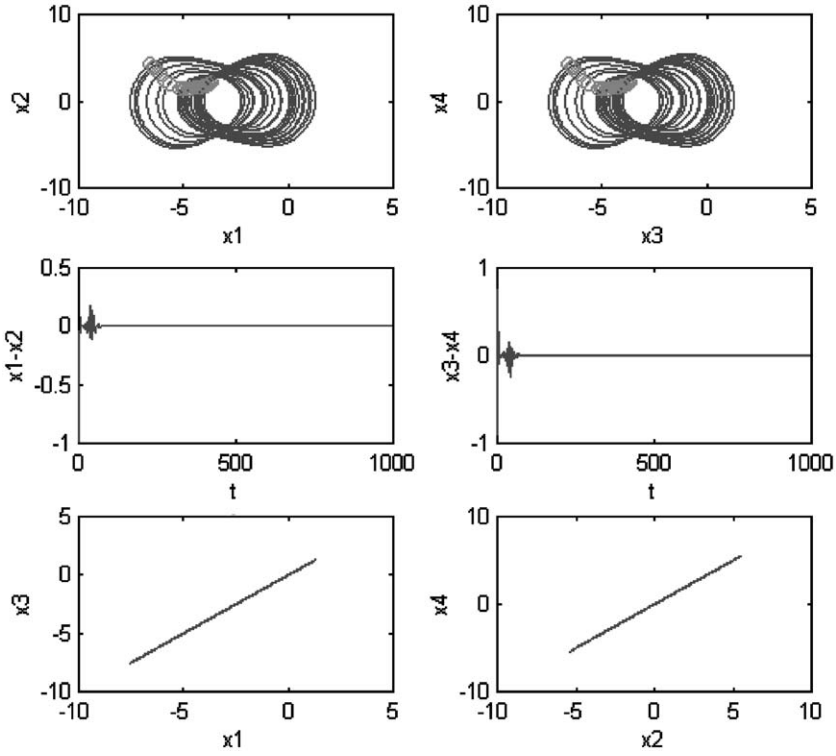

Fig. 3. Phase portraits, errors and similarity of unidirectional coupled systems with $k(x_1 - x_3)$, $k = 1.6$.

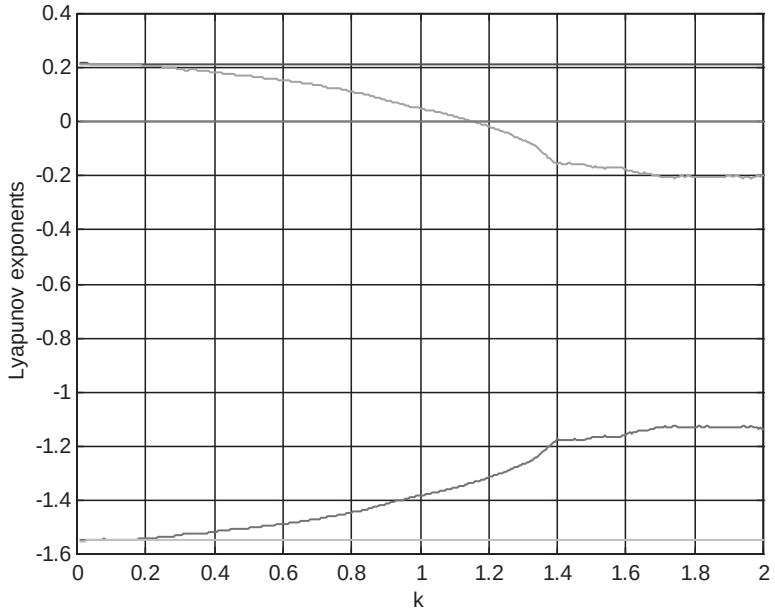

Fig. 4. Lyapunov exponent for k between 0 and 2.

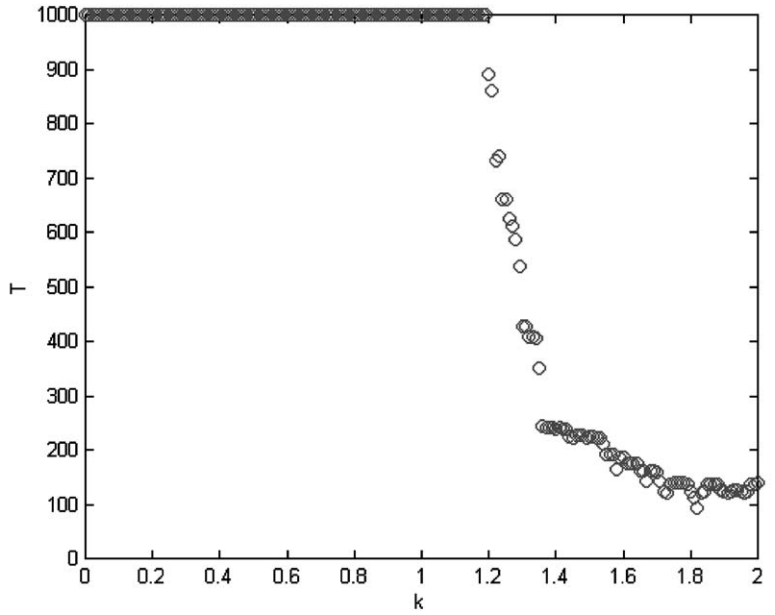

Fig. 5. Synchronization time for different k.

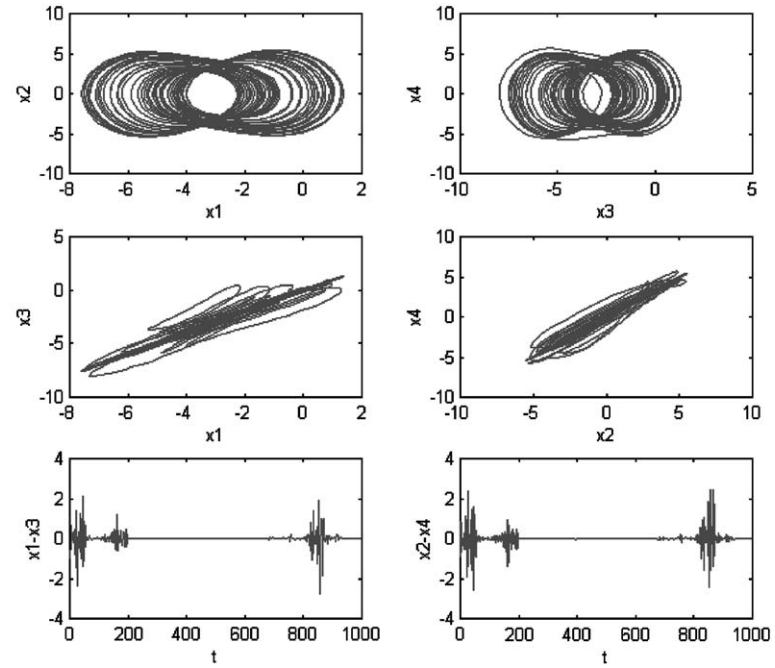

Fig. 6. Phase portraits, errors and similarity of unidirectional coupled systems with $k(x_1 - x_3)$, $k = 1.1$.

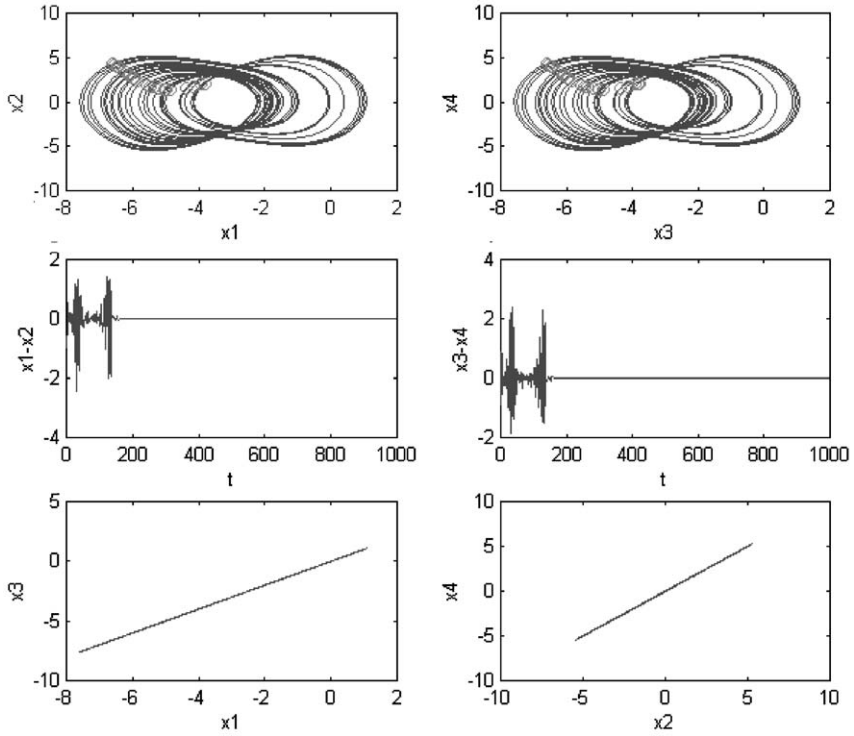

Fig. 7. Phase portraits, errors and similarity of unidirectional coupled systems with $k\sin(x_1 - x_3)$, $k = 1.3$.

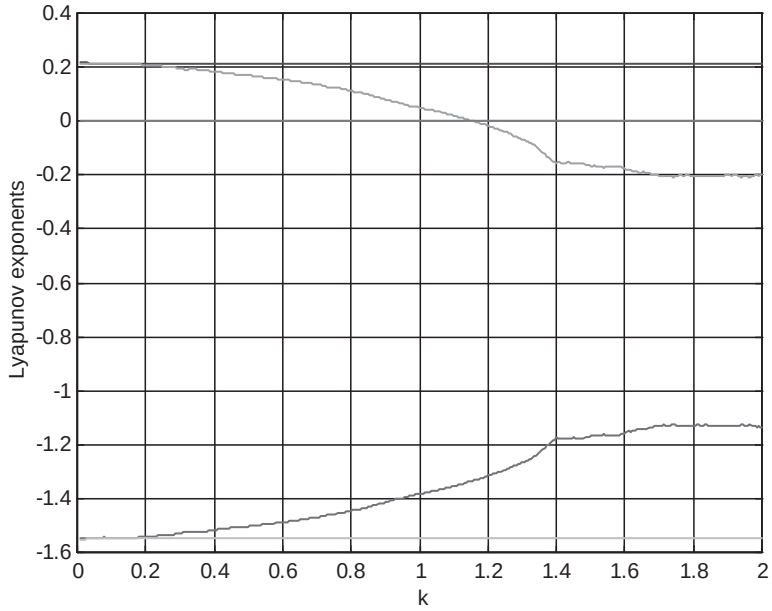

Fig. 8. Lyapunov exponent for k between 0 and 2.

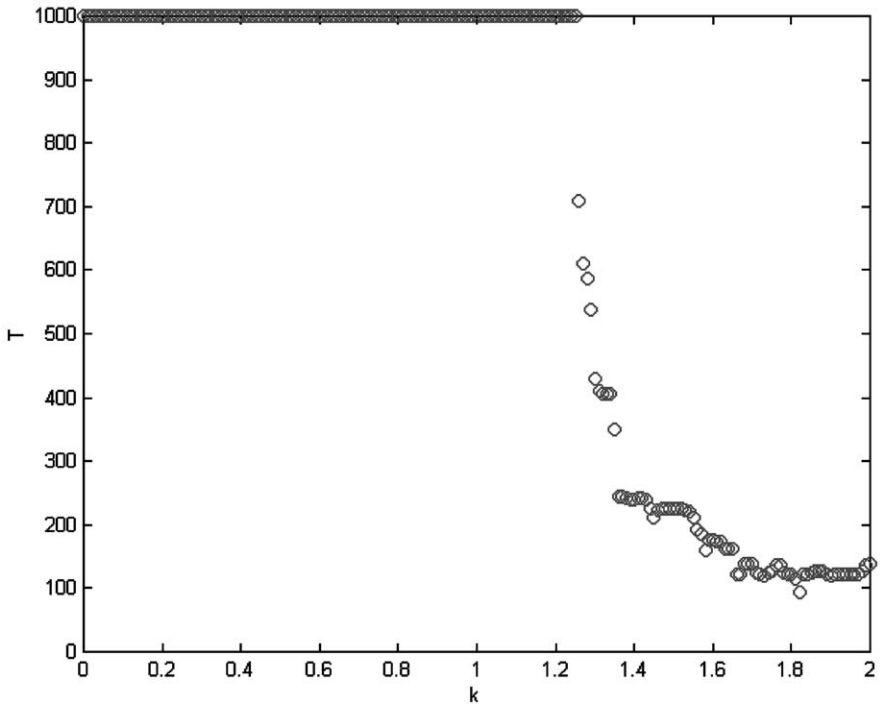

Fig. 9. Synchronization time for different k.

the Lyapunov exponent spectra corresponding to Figs. 22 and 23. It indicates that at $\varphi \approx 1$ and ≈ 1.3, the chaotic oscillation turns out to be periodic.

To determinate quantitatively the level of mismatch of chaos synchronization, we use similarity function $S(\tau)$ as a time averaged difference between the variables x_1 and x_3 taken with the time drift τ [6]

$$S^2(\tau) = \frac{\{[x_1(t+\tau) - x_3(t)]^2\}}{\left[\langle x_1^2(t)\rangle \langle x_3^2(t)\rangle\right]^{1/2}} \tag{5}$$

and plot the similarity function $S(0)$ versus φ; the result is plotted in Fig. 25. The increase of mismatch with the phase difference is linear for small φ.

In Fig. 26, we plot $S(\tau)$ versus τ with different coupling strength k. A minimum of $S(\tau)$ appears to be zero when $k > 1.2$.

Above all, we have considered the phase effect of the two mutually coupled systems. The phase difference plays an important role. Therefore, further increase of the phase difference even eliminates chaos and leads the coupled oscillators to periodic motion.

5. Transient time in unidirectional synchronization

In order to illustrate some observed characteristics in chaos synchronization, we take the linear coupled unidirectional systems ($F(x_3, x_1) = 0,\ F(x_1, x_3) = k(x_1 - x_3)$) for example. Our interest is

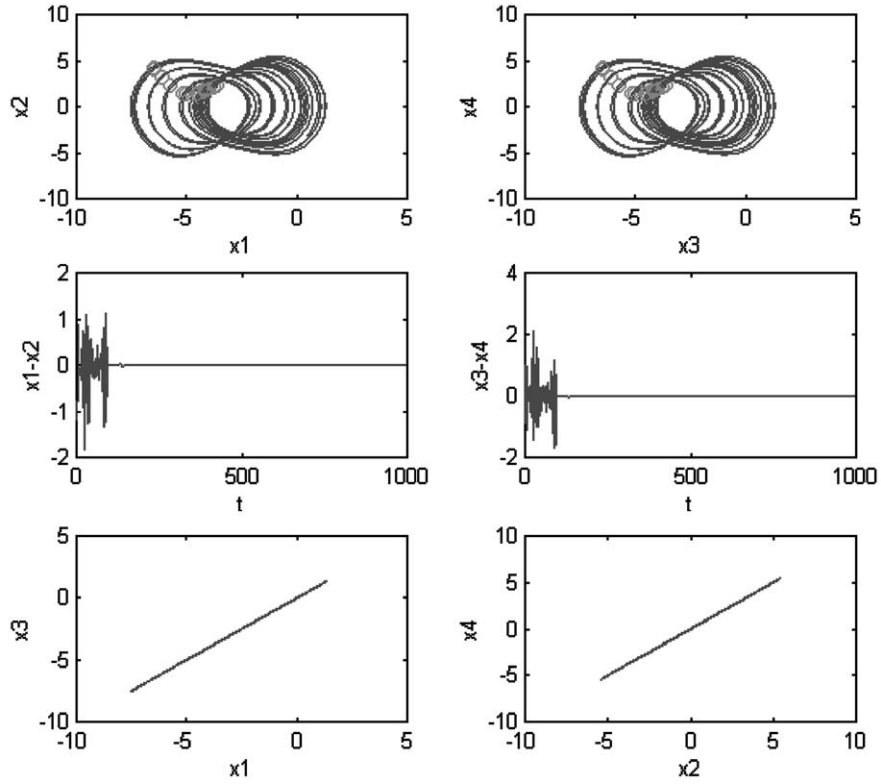

Fig. 10. Phase portraits, errors and similarity of unidirectional coupled systems with $k(e^{(x_1-x_3)}-1)$, $k=1.2$.

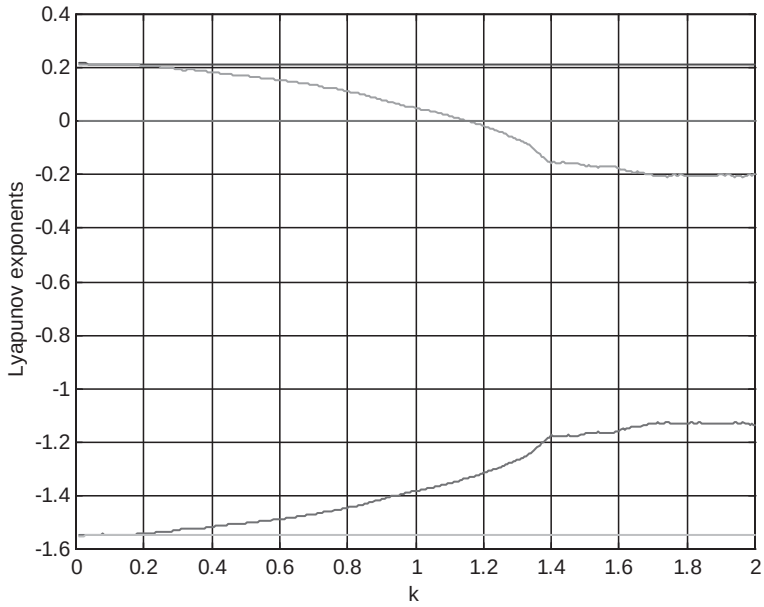

Fig. 11. Lyapunov exponent for k between 0 and 2.

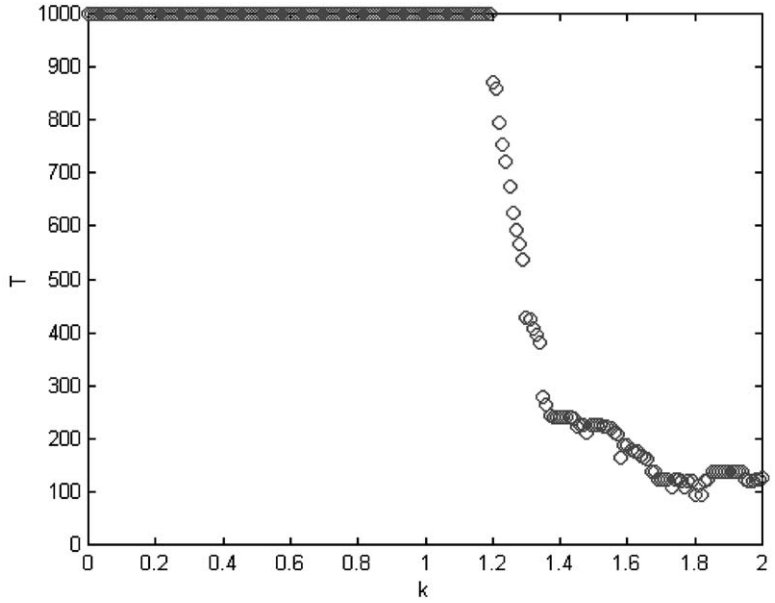

Fig. 12. Synchronization time for different k.

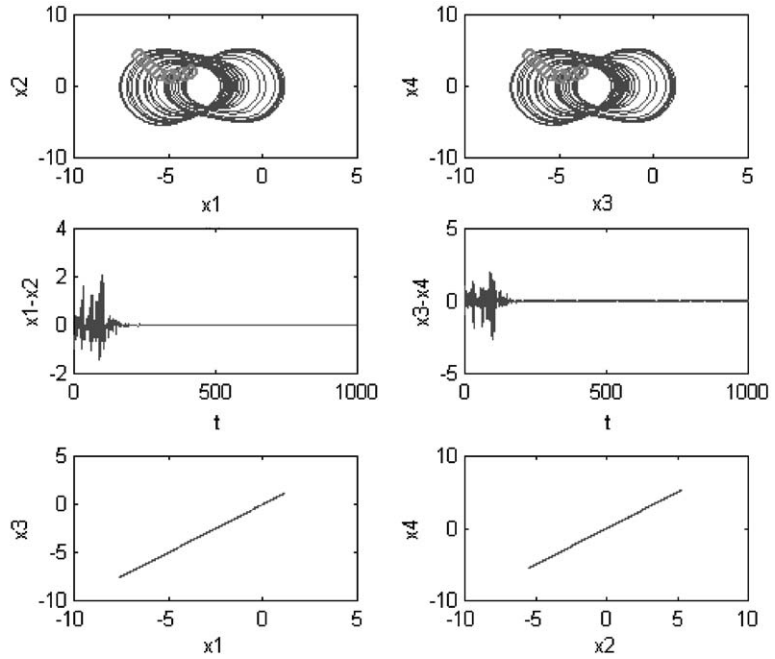

Fig. 13. Phase portraits, errors and similarity of bi-directional coupled systems with $F(x_3, x_1) = k[e^{(x_3-x_1)} - 1]$, $F(x_1, x_3) = k[e^{(x_1-x_3)} - 1]$, $k = 0.6$.

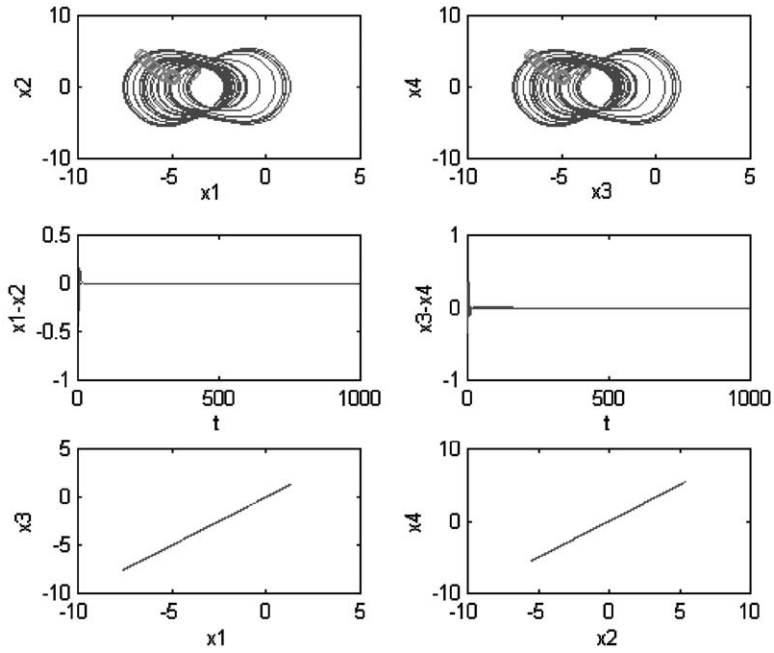

Fig. 14. Phase portraits, errors and similarity of bi-directional coupled systems with $F(x_3, x_1) = k[e^{(x_3-x_1)} - 1]$, $F(x_1, x_3) = k[e^{(x_1-x_3)} - 1]$, $k = 0.7$.

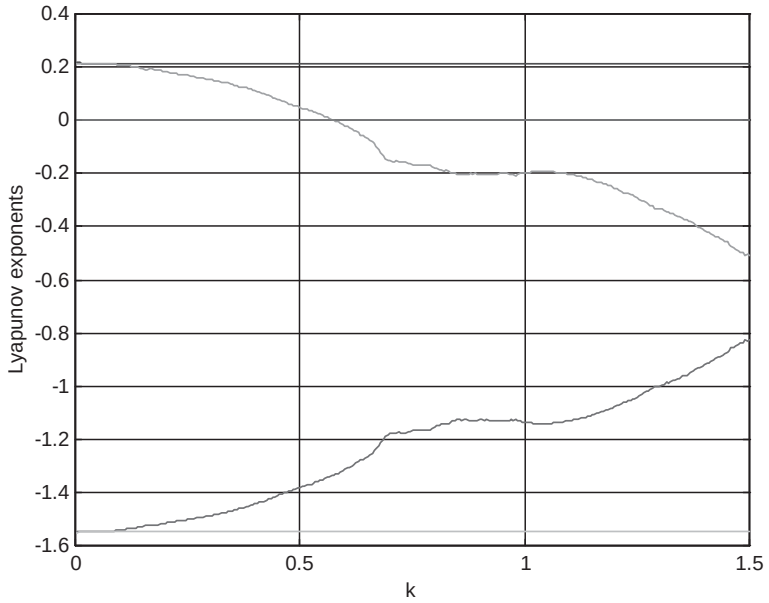

Fig. 15. Lyapunov exponent for k between 0 and 1.5.

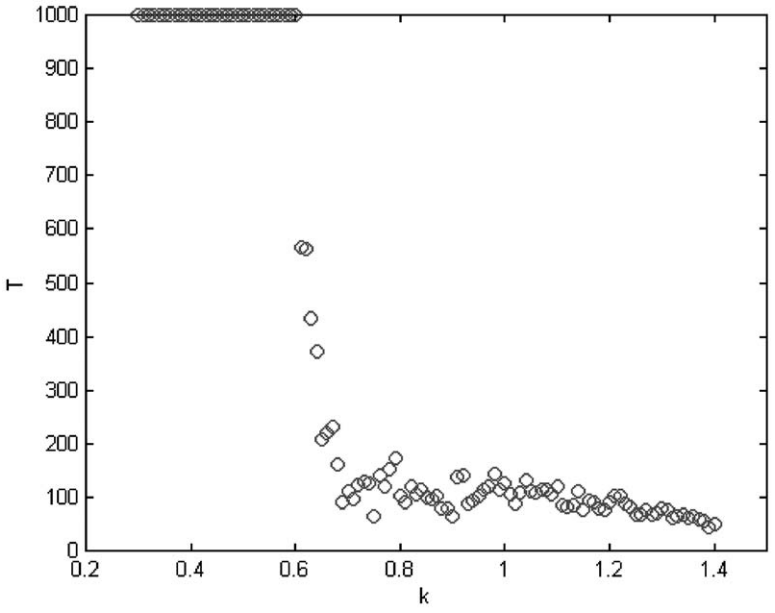

Fig. 16. Synchronization time for different k.

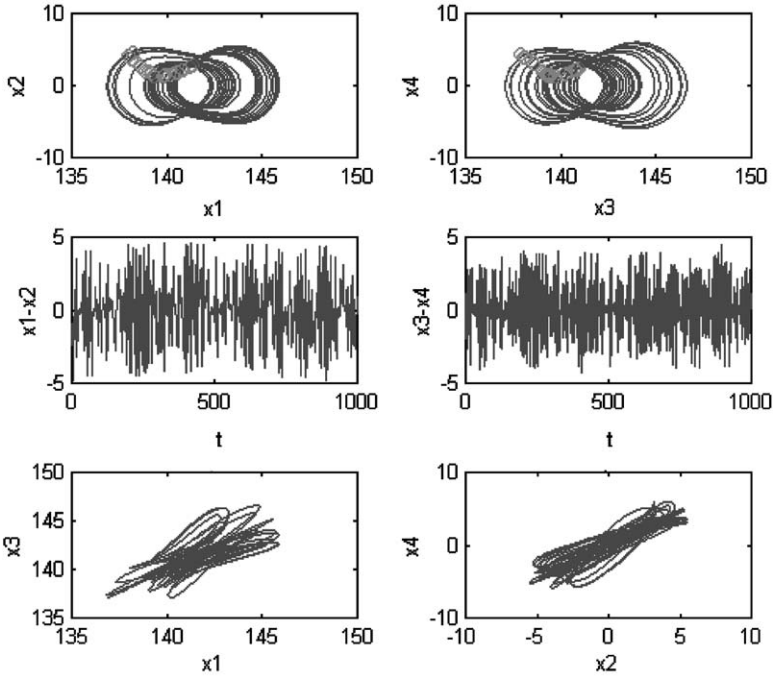

Fig. 17. Phase portraits, errors and similarity of bi-directional coupled systems with $F(x_3, x_1) = k[e^{(x_3-x_1)} - 1]$, $F(x_1, x_3) = k[e^{(x_1-x_3)} - 1]$, $k = 0.05$.

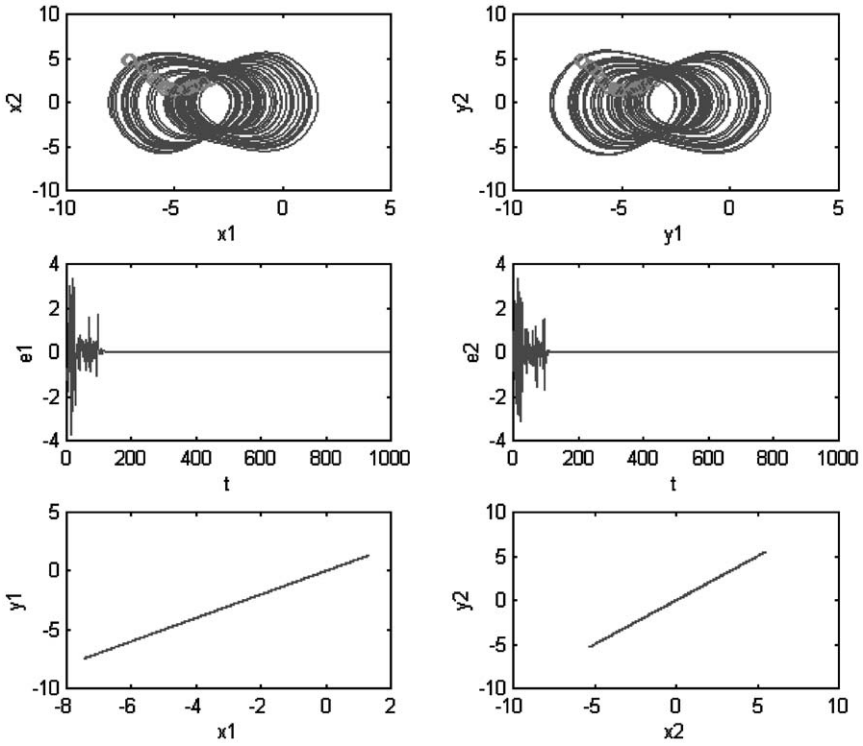

Fig. 18. Phase portraits, errors and similarity of bi-directional coupled systems with $F(x_3, x_1) = k \sin[e^{(x_3 - x_1)} - 1]$, $F(x_1, x_3) = k \sin[e^{(x_1 - x_3)} - 1]$, $k = 0.6$.

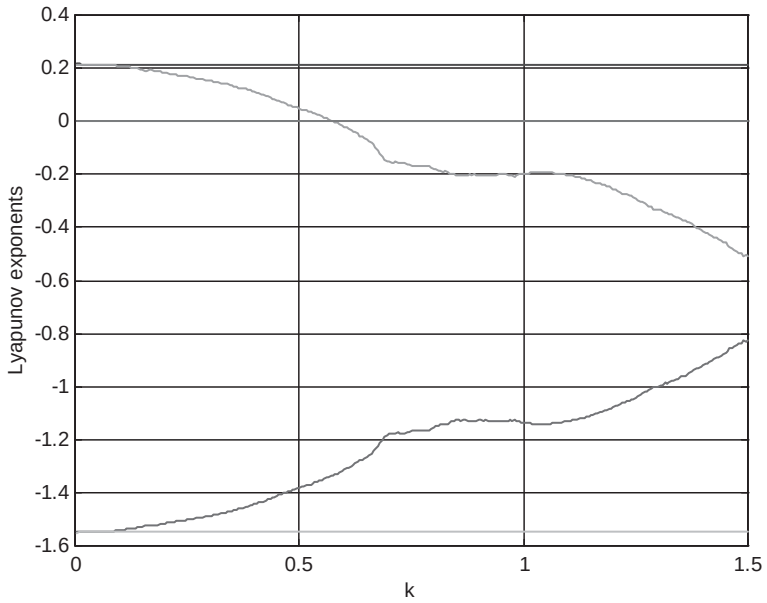

Fig. 19. Lyapunov exponent for k between 0 and 1.5.

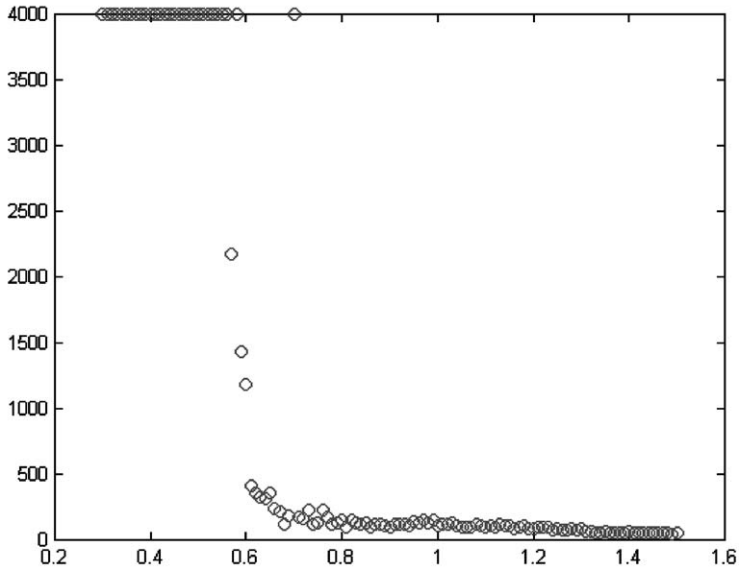

Fig. 20. Synchronization time for different k.

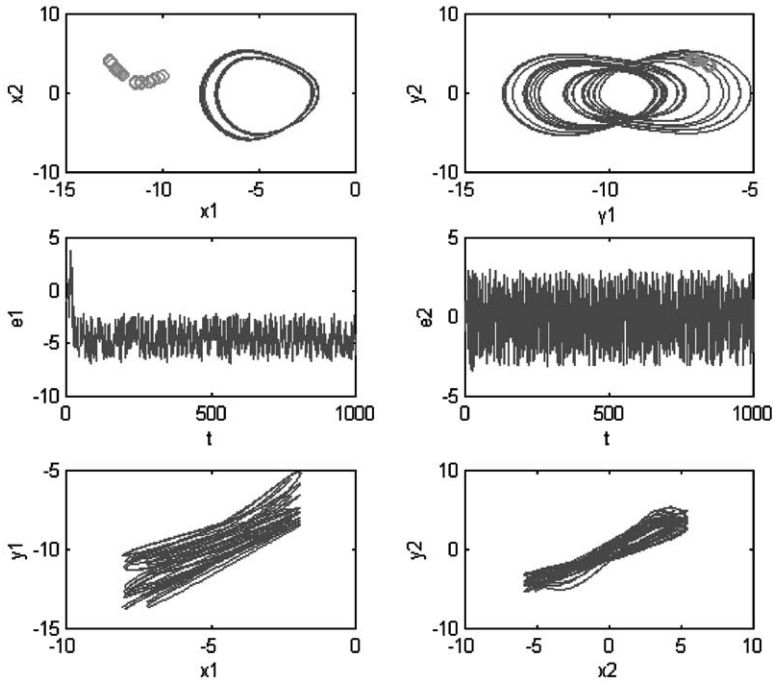

Fig. 21. Phase portraits, errors and similarity of bi-directional coupled systems with $F(x_3, x_1) = k \sin[e^{(x_3 - x_1)} - 1]$, $F(x_1, x_3) = k \sin[e^{(x_1 - x_3)} - 1]$, $k = 0.7$.

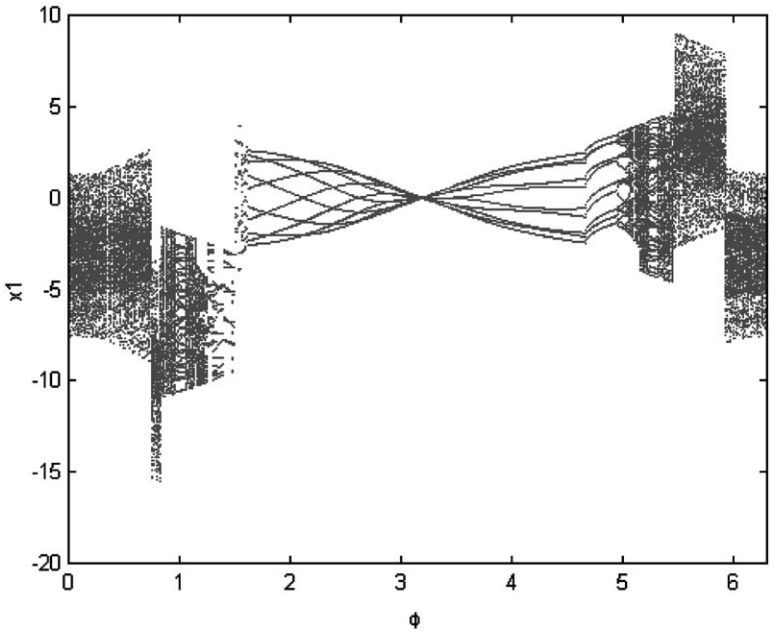

Fig. 22. Bifurcation diagram for φ between 0 and 2π versus $x_{1.}$

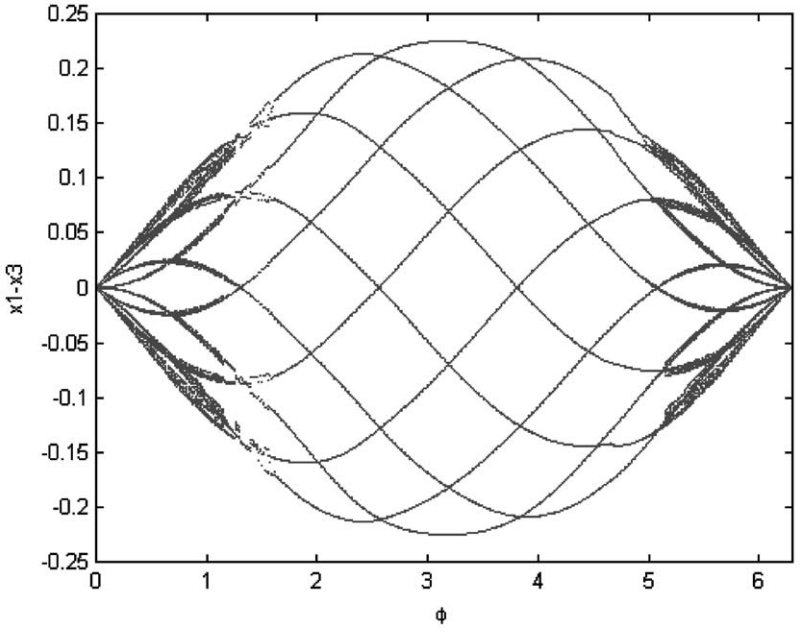

Fig. 23. Bifurcation diagram for φ between 0 and 2π versus error.

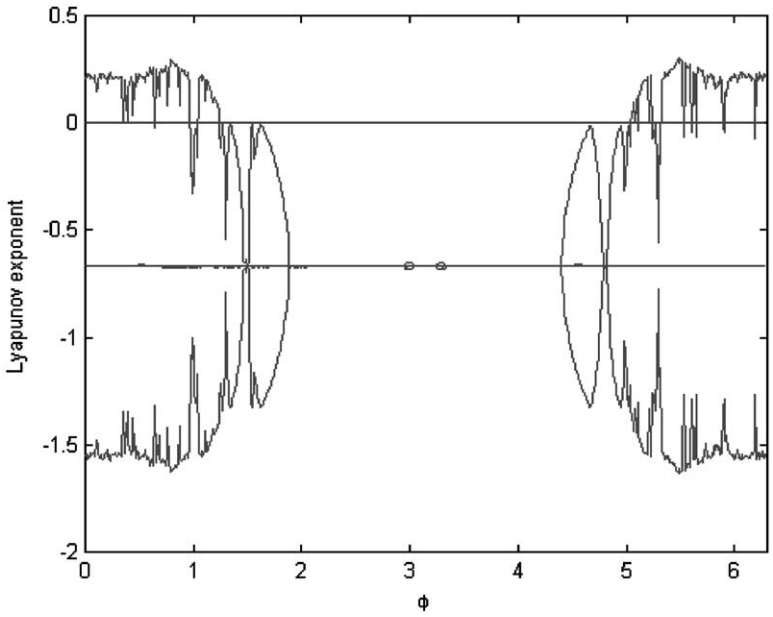

Fig. 24. Lyapunov exponent for φ between 0 to 2π.

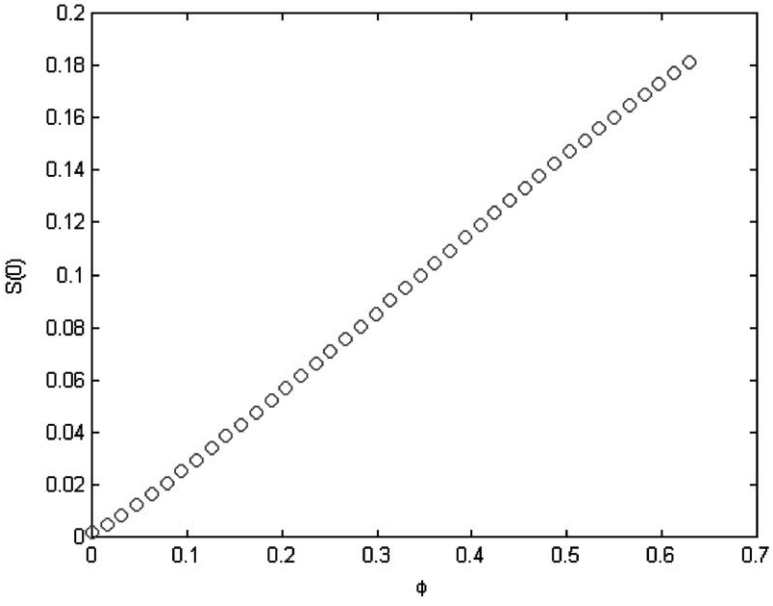

Fig. 25. Similarity function $S(0)$ versus the phase differenceφ.

focused on the behavior of the system when it is in chaotic state with values of the coupling parameter which lead to synchronization, and in the time of transient decay onto the synchronized state.

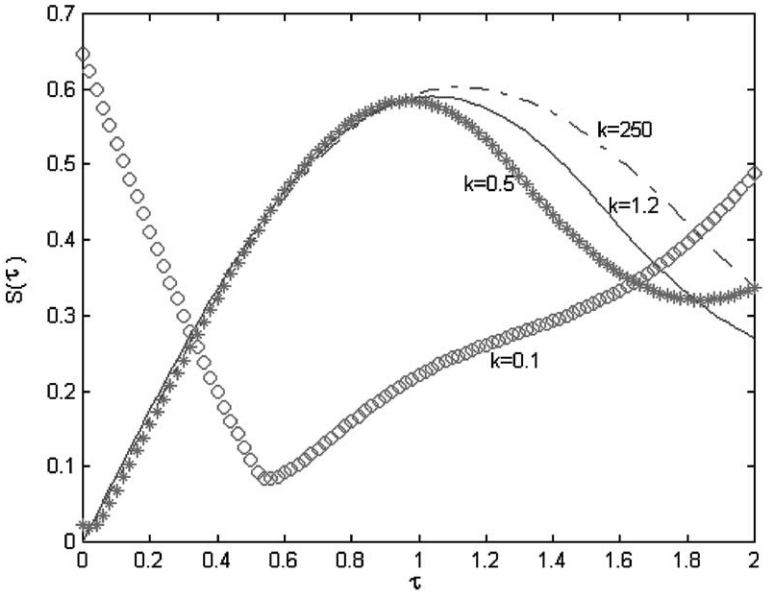

Fig. 26. Similarity function $S(\tau)$ for different values of coupling strength k.

The Euclidean distance $d = \sqrt{(x_1 - x_3)^2 + (x_2 - x_4)^2}$ between two trajectories is monitored for various choices of the coupling parameter k as shown in Fig. 27. Increasing the value of the coupling parameter, we see that the transition to the synchronized state occurs at $k_c \cong 1.4$ for this numerical simulation, after which systems (2) and (3) display the same output. For the value of k greater than k_c the synchronized state is stable. The length of transient time may depend on the coupling parameter and on the initial conditions. In Fig. 28, we plot three typical curves representing the full evolution of $\mathrm{d}(t)$. The three curves are computed for identical initial conditions. The evolution of $\mathrm{d}(t)$ when $k = 1.2$ can be notionally split into two different parts. The first evolution τ_o is the *orbiting transient*, and the second part τ_d is the *decaying transient* [7]. From Fig. 28, we can see that as the value of k increases, the transient time decreases.

6. Conclusion

During the past decade, there are many effective methods that can be used for chaos synchronization. Synchronized chaotic systems can be used as cipher generators for secure communication, symmetry and pattern formation, and self-organization. It is worthy of researching. Synchronization of subsystem is studied by employing a continuous feedback method. Varying coupling strength, the motion of subsystems become to synchrony. Besides, we can see how phase difference of external excitations affects the synchronization. Then we have observed the transient time in synchronization, which helps us to understand more about synchronization.

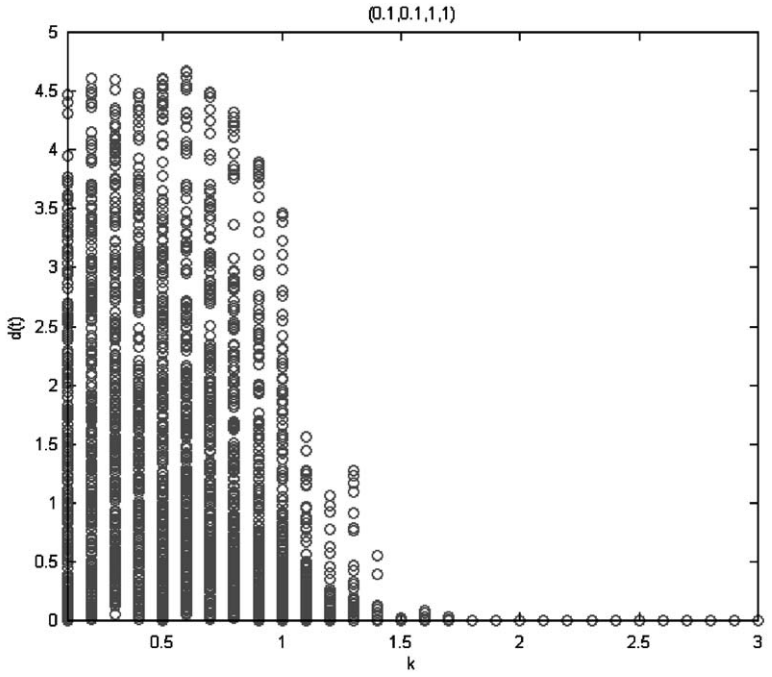

Fig. 27. Plot of several values of the Euclidean distance d(t) between the trajectories (x_1, x_2, x_3, x_4) for different values of k.

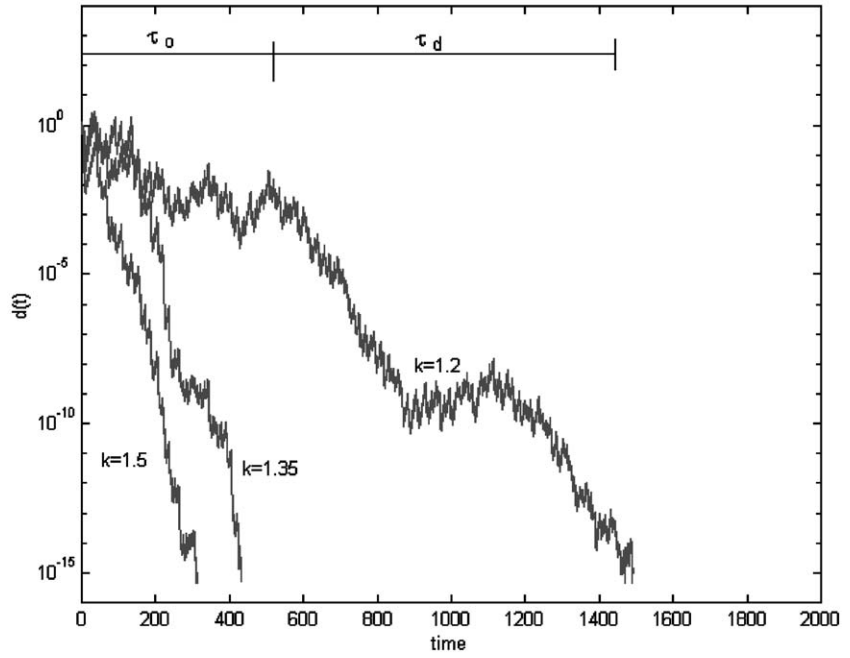

Fig. 28. Two curves representing the time evolution of Euclidean distance d(t) between the drive and the response trajectories.

Acknowledgements

This research was supported by the National Science Council, Republic of China under grant number NSC 91-2212-E-009-025.

References

[1] L. Kocarev, General approach for chaotic synchronization with applications to communication, Physical Review Letters 74 (1995) 5028.
[2] M. Lakshmanan, K. Murali, Chaos in Nonlinear Oscillators: Controlling and Synchronization, World Scientific, Singapore, 1996.
[3] Hua-Wei Yin, Jian-Hua Dai, Hong-Jun Zhang, Phase effect of two coupled periodically driven duffing oscillators, Physical Review E 58 (1998) 5683.
[4] Chien-Lung Huang, Nonlinear Dynamics of the Horizontal Platform, Master of Science in Mechanical Engineering Thesis, NCTU, 1996.
[5] G. Chen, X. Dong, From Chaos To Order: Methodologies, Perspectives and Applications, World Scientific, Singapore, 1998.
[6] M.G. Rosenblum, A.S. Piskovsky, J. Kurths, From phase to lag synchronization in coupled chaotic oscillators, Physical Review Letters 78 (1997) 4193.
[7] G. Savtoboni, S.R. Bishop, Transient time in unidirectional synchronization, International Journal of Bifurcation and Chaos in Applied Sciences and Engineering 9 (12) (1999) 2345.